HHS Public Access

Author manuscript

Mol Microbiol. Author manuscript; available in PMC 2016 December 01.

Published in final edited form as:

Mol Microbiol. 2015 December ; 98(5): 895–909. doi:10.1111/mmi.13164.

MinC/MinD copolymers are not required for Min function

Kyung-Tae Park, **Shishen Du**, and **Joe Lutkenhaus***

Department of Microbiology, Molecular Genetics and Immunology, University of Kansas Medical Center, Kansas City KS 66160

Summary

In *Escherichia coli*, precise placement of the cytokinetic Z ring at midcell requires the concerted action of the three Min proteins. MinD activates MinC, an inhibitor of FtsZ, at least in part, by recruiting it to the membrane and targeting it to the Z ring, while MinE stimulates the MinD ATPase inducing an oscillation that directs MinC/MinD activity away from midcell. Recently, MinC and MinD were shown to form copolymers of alternating dimers of MinC and MinD and it was suggested that these copolymers are the active form of MinC/MinD. Here, we use MinD mutants defective in binding MinC to generate heterodimers with wild type MinD that are unable to form MinC/MinD copolymers. Similarly, MinC mutants defective in binding to MinD were used to generate heterodimers with wild type MinC that are unable to form copolymers. Such heterodimers are active and in the case of MinC were shown to mediate spatial regulation of the Z ring demonstrating that MinC/MinD copolymer formation is not required. Our results are consistent with a model in which a membrane anchored MinC/MinD complex is targeted to the Z ring through the conserved carboxy tail of FtsZ leading to breakage of FtsZ filaments.

Keywords

Z ring; MinC; MinD; copolymer

Introduction

Prokaryotic cytokinesis is initiated by formation of the Z ring, a cytoskeletal element that recruits downstream division proteins to form the divisome, which carries out cell division (Lutkenhaus, 2007, de Boer, 2010, Shih & Rothfield, 2006, Margolin, 2005, Bi & Lutkenhaus, 1991, Lutkenhaus *et al.*, 2012). The position of the cytokinetic Z ring is restricted to midcell by the combined action of two negative regulators in model rod-shaped organisms such as *Bacillus subtilis* and *Escherichia coli*. One is nucleoid occlusion that prohibits Z ring assembly over unsegregated chromosomes (Wu & Errington, 2004, Bernhardt & de Boer, 2005, Tonthat *et al.*, 2011, Du & Lutkenhaus, 2014). The second is the Min system that blocks Z ring assembly away from midcell. In *E. coli* the Min system consists of three proteins, MinC, MinD, and MinE. MinC and MinD form an inhibitory complex at the membrane that suppresses Z ring formation (de Boer *et al.*, 1989, Johnson *et al.*, 2002, Hu *et al.*, 2003, Hu *et al.*, 1999). In the presence of MinE, MinC/MinD undergo an

*Corresponding author: Tel: (913) 588-7054, FAX: (913) 588-7295, jlutkenh@kumc.edu.

oscillation such that the time-averaged concentration of MinC/MinD on the membrane is lowest at midcell (Raskin & de Boer, 1999, Hu & Lutkenhaus, 1999, Meinhardt & de Boer, 2001).

MinD is a member of the WACA (walker A cytomotive ATPase) family that is characterized by the deviant walker A motif, which also includes the ParA-like proteins implicated in partition of macromolecules including DNA (Lutkenhaus & Sundaramoorthy, 2003, Lowe & Amos, 2009, Ebersbach & Gerdes, 2005). Members of this family share several biochemical features. The ATP-bound form adheres to the surface of a matrix, the membrane for MinD and the DNA for ParA. In the presence of a partner protein that stimulates ATP hydrolysis, MinE for MinD and ParB for ParA, these proteins exhibit dynamic oscillatory behavior, which transports cognate cargo molecules, MinC for MinD and ParB bound plasmids for ParA (Lutkenhaus, 2012, Gitai, 2006, Szardenings *et al.*, 2011, Vecchiarelli *et al.*, 2012, Hu & Lutkenhaus, 2001). Importantly, this behavior leads to spatial regulation of the cargo. The interaction between MinD and MinE sets up a gradient of MinC/MinD on the membrane that is highest at the poles and lowest at midcell, where the Z ring forms (Meinhardt & de Boer, 2001). Several WACA proteins have purportedly been shown to undergo ATP-dependent polymerization *in vitro* (Ebersbach & Gerdes, 2004, Leonard *et al.*, 2005, Ivanov & Mizuuchi, 2010, Hu *et al.*, 2002, Suefuji *et al.*, 2002), however, this is controversial and reexamination of such assemblies by electron microscopy indicates they are artifacts (Ghosal *et al.*, 2014).

MinC is comprised of two distinct functional domains both of which interact with FtsZ. The N-terminal domain ($MinC^N$) is sufficient to inhibit FtsZ ring formation *in vivo* when overexpressed and to antagonize FtsZ polymerization *in vitro* (Hu *et al.*, 1999, Hu & Lutkenhaus, 2000). Genetic evidence indicates this domain interacts with the H10 helix of FtsZ (Shen & Lutkenhaus, 2010). The C-terminal domain ($MinC^C$) mediates dimerization, binding to MinD and interaction with the C-terminal tail of FtsZ (Hu & Lutkenhaus, 2000, Shen & Lutkenhaus, 2009, Szeto *et al.*, 2001, Zhou & Lutkenhaus, 2005, Ramirez-Arcos *et al.*, 2004), also called the conserved carboxy-terminal peptide (CCTP) (Du *et al.*, 2015). Although $MinC^C$ prevents bundling of FtsZ polymers *in vitro* (Dajkovic et al. 2008), efficient interaction of $MinC^C$ with the CCTP *in vivo* requires MinD since $MinC^C$ is only targeted to the Z ring in the presence of MinD (Hu *et al.*, 2003, Johnson *et al.*, 2002). Overexpression of $MinC^C$ in the presence of MinD results in competition with FtsA and ZipA for the CCTP of FtsZ leading to disruption of the Z ring (Shen & Lutkenhaus, 2009, Shiomi & Margolin, 2007). On the basis of the above observations it was suggested that the two domains of MinC act synergistically; the interaction of $MinC^C$/MinD with the CCTP places $MinC^N$ in close proximity to FtsZ polymers FtsZ (Shen & Lutkenhaus, 2010).

Although MinC is the actual inhibitor and contacts FtsZ directly, MinD is required for MinC to be fully active *in vivo* (de Boer *et al.*, 1992). This activation is due to MinD concentrating MinC at the membrane and targeting MinC to the Z ring (Hu *et al.*, 2003, Johnson *et al.*, 2002). Although the addition of a membrane anchor to MinC enhances its inhibitory activity, such constructs are further activated by the addition of MinD (Johnson *et al.*, 2004). Also, MinC can be partially activated by a MinD mutant unable to bind the membrane. It is

likely that this MinD mutant targets MinC directly to the Z ring but is less efficient than wild type MinD (Hu & Lutkenhaus, 2003).

Recently, Ghosal *et al.* reported that MinC and MinD form copolymers and proposed that these copolymers are the active form of MinC/MinD that regulates Z ring assembly (Ghosal *et al.*, 2014). Using sedimentation and electron microscopy they found that copolymers formed *in vitro* in an ATP dependent manner. Combining their structure of the *Aquifex aeolicus* MinC/MinD complex (MinD-$MinC_2$-MinD) with that of the *E. coli* MinD dimer they built a composite filament model of alternating dimers of MinC and MinD that matched the axial repeat distance of negatively stained MinC/MinD filaments (Fig. 1A). Although polymerization displayed a long lag and high critical concentration, it was suggested that these could be reduced *in vivo* by the presence of the membrane. Conti *et al.* also reported that MinC and MinD form filaments in the presence of ATP (Conti *et al.*, 2015). They did not observe a critical concentration and assembly was reduced by pH and salt concentrations that resembled physiological conditions.

The oscillation of MinD and MinE occurs whether or not MinC is present (Hu & Lutkenhaus, 1999, Raskin & de Boer, 1999), indicating MinC/MinD copolymers have no role in the oscillation. Ghosal *et al.* (Ghosal *et al.*, 2014) pointed out that MinC/MinD copolymers should preferably interact with FtsZ filaments over FtsZ monomers due to avidity. Also, their failure to observe inhibition of FtsZ assembly by MinC *in vitro* led them to suggest that MinC/MinD copolymers were indeed the active inhibitory complex and proposed they function by altering the structural integrity of FtsZ filaments or the interaction between FtsZ and FtsA filaments. In this study we used genetic tests to determine whether MinC/MinD copolymers are critical for MinC/MinD regulation of the Z ring using MinC and MinD mutants defective in forming MinC/MinD copolymers.

Results

Strategy of using heterodimers to examine the role of MinC/MinD copolymers

Ghosal *et al.* (Ghosal *et al.*, 2014) previously showed that a MinD mutant, $MinD^{D154A}$ (Zhou *et al.*, 2005, Ma *et al.*, 2004) incapable of forming copolymers, was unable to convert a Δ*min* strain to wild type phenotype in the presence of MinC and MinE. However this is not a critical test for the model, since $MinD^{D154A}$ fails to uncouple MinC binding from MinC/MinD copolymerization. In other words, the failure of MinC/$MinD^{D154A}$/MinE to rescue a Δ*min* phenotype is simply a result of the loss of MinC binding by $MinD^{D154A}$ and not a specific test for the role of the MinC/MinD copolymer. To examine the possibility that MinC/MinD copolymers made up of alternating dimers of MinC and MinD are essential for inhibiting cell division and spatial regulation of the Z ring, and to overcome the problem associated with $MinD^{D154A}$ above, we explored the activity of MinD heterodimers *in vivo*. In this approach a MinD mutant like $MinD^{D154A}$ was over-expressed in a strain containing wild type MinD and MinC. This should lead to the formation of MinD heterodimers *in vivo* which can bind MinC on only one side of the heterodimer (Fig. 1B). Such a heterodimer could possibly still recruit MinC to the membrane but would be unable to polymerize. Similarly, over-expression of a MinC mutant unable to interact with MinD along with wild type MinC and MinD should result in MinC heterodimers (Fig. 1D). The over-expression of

such a MinC mutant should sequester the wild type MinC in heterodimers with the excess MinC mutant forming homodimers. The heterodimers could still be recruited to the membrane by interaction with MinD (MinD can interact with the WT subunit in the heterodimer) but could not form copolymers since MinD could only bind to one side of the dimer. The excess homodimers of the MinC mutant are relatively nontoxic as they cannot be recruited to the membrane and would have to be over expressed ~40 fold before they would become toxic (de Boer *et al.*, 1992).

Formation of MinD heterodimers defective in copolymer formation does not undermine MinC/MinD-dependent cell division inhibition

To test the importance of copolymers of MinC/MinD in regulating FtsZ we tested the effect of a MinD heterodimer on MinC/MinD activity. To do this, a MinD mutant ($MinD^{D154A}$) defective in MinC binding was expressed in the presence MinC/MinD (Fig. 1B). A plasmid containing an IPTG-inducible $MinD^{D154A}$ (pZH115 [P*tac:: minD*^{D154A}]) was introduced in a Δ*min* strain (JS964) along with a compatible plasmid encoding wild type MinC/MinD that is arabinose-inducible (pSEB104CD [P*ara:: minC minD*]). This latter plasmid produces about four times the physiological level of MinC/MinD (Fig. S1) and inhibits colony formation when induced with 0.2% arabinose (Fig. 2A, row 2) (Zhou & Lutkenhaus, 2005). This inhibition is suppressed by coexpression of MinE as expected (Fig. 2A, row 1). When $MinD^{D154A}$ is coexpressed with MinC/MinD heterodimers with wild type MinD should form such that a wild type MinC dimer could only bind to one side of the MinD heterodimer. As a result the largest species that could form is a MinC dimer flanked by MinD heterodimers (Fig. 1B). The expression of $MinD^{D154A}$ along with MinC/MinD in JS964 (Δ*min*) did not prevent the inhibition of colony formation (Fig. 2A, rows 2 and 4) suggesting the MinD:$MinD^{D154A}$ heterodimer is active. A control in which $MinD^{D154A}$ was expressed along with MinC/$MinD^{D154A}$ did not inhibit growth confirming that $MinD^{D154A}$ does not activate MinC (data not shown). Together, these results suggest that MinC flanked by MinD heterodimers is sufficient to inhibit division.

The $MinD^{D154A}$ mutant must dimerize since it is able to bind MinE and the membrane, both of which require dimerization (Zhou, Schulze et al. 2005). However, to demonstrate that the *minD*^{D154A} mutation did not affect dimerization with MinD *in vivo*, we introduced another substitution, $MinD^{T91K}$ (Wu *et al.*, 2011), on the opposite side of $MinD^{D154A}$ to create a double mutant, $MinD^{T91K/D154A}$. One mutation disrupts MinC binding on one side of the dimer whereas the other disrupts the MinC binding site on the opposite side of the dimer. A heterodimer formed between this double mutant and wild-type MinD would be unable to bind MinC since the MinC binding sites on both sides of the heterodimer are disrupted (Fig. 1C). Therefore, such a double mutant should be dominant negative and inactivate MinC/MinD so that division, and therefore colony formation, should no longer be inhibited. Consistent with this prediction, and in contrast to what was observed with $MinD^{D154A}$, expression of $MinD^{T91K/D154A}$ largely prevented MinC/MinD from inhibiting colony formation (Fig. 2A, row 5), providing evidence the MinD mutants indeed formed a heterodimer with MinD.

To demonstrate that MinD^{D154A} can dimerize with MinD *in vitro*, we performed a copelleting assay using ultracentrifugation after confirming that MinD^{D154A} was unable to recruit MinC to vesicles (Fig. S2). The rationale was that the formation of MinD^{D154A}:MinD heterodimers would block MinC and MinD from forming copolymers in the presence of ATP. The addition of excess MinD^{D154A} to the MinC/MinD reaction should yield two dimeric species of MinD. One is the heterodimer that can still bind to MinC via the one active site and the other is MinD^{D154A} homodimers, which cannot bind to MinC. Hence, the only oligomeric MinC/MinD species, if any, will be a trimeric complex in which a MinC dimer is flanked by two MinD heterodimers (Fig. 1B), which will not pellet under these conditions. Consistent with the previous reports MBP-MinC^{C} and MinD copelleted in an ATP dependent fashion indicative of copolymer formation (Fig. 2B, lane 2) (Ghosal *et al.*, 2014). However, when an excess of MinD^{D154A} was coincubated with MinC/MinD the pelleting efficiency was reduced to background levels (Fig. 2B, lane 4). These results confirm that the MinD^{D154A} forms heterodimers with MinD and that MinD^{D154A}/MinD heterodimers prevent copolymer formation.

Expression of a MinC mutant unable to bind MinD does not significantly compromise MinC/MinD activity

To support the above results obtained with the MinD mutant we tested if a MinC heterodimer unable to form copolymers with MinD could still inhibit cell division (Fig. 1D). Similar to the approach above, a plasmid containing an IPTG-inducible MinC^{R133A} (pJF118EH-C [P*tac:: minC^{R133A}*]) was introduced in a Δ*min* strain (JS964) along with a compatible plasmid encoding wild type MinC/MinD that is arabinose-inducible (pSEB104CD [P*ara:: minC minD*]). The *minC^{R133A}* mutation, which changes the arginine residue to alanine in the conserved ^{133}RSGQ^{136} motif in the C-terminal domain of MinC, was previously shown to abrogate MinD binding (Zhou *et al.*, 2005, Ma *et al.*, 2004). Induction of MinC^{R133A} alone (Fig. 3A, row 2) or with MinC^{R133A}/MinD (Fig. 3A, row 3) did not block colony formation demonstrating that this level of expression is nontoxic and that MinD was unable to activate MinC^{R133A}. When MinC^{R133A} was coexpressed with MinC/MinD, the inhibition of colony formation by MinC/MinD was not affected (Fig. 3A, compare rows 4 and 5). When MinC/MinD was induced with less arabinose (0.005%) growth was reduced and this was not affected by coexpression of MinC^{R133A} (Fig. 3A) Western analysis revealed that the MinC^{R133A} level at 10 μM IPTG was ~15 times the level of MinC induced by 0.2% arabinose (Fig. S1), sufficient to convert all of MinC^{WT} to heterodimers (MinC^{WT}:MinC^{R133A}). Under these conditions the largest MinC/MinD complex that could form would be a tripartite complex composed of a MinD dimer flanked by MinC heterodimers (MinC^{R133A}:MinC/MinD$_2$/MinC:MinC^{R133A}). It is doubtful such a complex forms, however, since MinD is estimated to be in sevenfold excess over MinC in wild type cells (Li *et al.*, 2014). Furthermore, these results suggest that a MinD dimer bound to one side of a MinC dimer is sufficient to recruit it to the membrane and activate it.

Confirmation of heterodimer formation by MinC mutants—Consistent with published results (Zhou & Lutkenhaus, 2005), the *minC^{R133A}* mutation did not affect the stability of MinC (Fig. S1). However, to confirm that MinC^{R133A} dimerized with the wild type protein *in vivo* two tests were conducted. First, a bacterial 2-hybrid test demonstrated

that MinC interacted with WT MinC as well as another MinC mutant (Fig. S3). Second, an experiment was devised where dimerization was required to rescue MinC activity. In this experiment two MinC mutants, each with a lesion in a different domain, were coexpressed to see if inhibitory activity could be restored. $MinC^{G10D}$, which has a defect in the $MinC^{N}$ domain (Hu *et al.*, 1999), was expressed along with $MinC^{R133A}$, which reduces the ability of the $MinC^{C}$ domain to bind MinD (Fig. 1E). Expression of $MinC^{R133A}$ or expression of $MinC^{G10D}$ with MinD did not inhibit colony formation (Fig. 3B, rows 2 and 3). However, coexpression of $MinC^{R133A}$ with $MinC^{G10D}$/MinD restored inhibitory activity as colony formation was prevented (Fig. 3B, row 4). Although there was some residual growth in the presence of the MinC heterodimer and MinD the cells were highly filamentous (data not shown). Thus, the heterodimer retains activity but appears slightly less active than the wild type dimer (Fig. 3B, row 5). This slight reduction in the activity of the $MinC^{R133A}$:$MinC^{G10D}$ heterodimer compared to the $MinC^{R133A}$:MinC heterodimer was confirmed in additional spot tests (Fig. S4A). Nonetheless, the results indicate that MinD binding to the C-terminal domain of one subunit is sufficient to recruit a MinC dimer to the membrane and activate the N-terminal domain of the other subunit in the dimer.

To further confirm that a MinC heterodimer having only one functional $MinC^{N}$ domain and one functional $MinC^{C}$ domain has cell division inhibitory activity we used a mutant MinC that lacked $MinC^{N}$. $MinC^{C}$ ($MinC^{125–231}$) was cloned into the pQE80L vector and expressed in strain JS964 that harbors a plasmid expressing MinD along with a MinC mutant, $MinC^{R172A}$, deficient in septal localization. This mutant has a functional $MinC^{N}$ domain and can bind MinD but does not localize to the Z ring due to the *minC*^{R172A} mutation preventing interaction of $MinC^{C}$ with the CCTP of FtsZ (Zhou & Lutkenhaus, 2005). The resultant heterodimer, however, can be targeted to the CCTP by MinD binding to the $MinC^{C}$ subunit (Fig. 1F). Coexpression of $MinC^{C}$ and $MinC^{R172A}$/MinD suppressed colony formation indicating the heterodimer ($MinC^{C}$/$MinC^{R172A}$) was active (Fig. 3C, row 4). Although expression of $MinC^{C}$ alone does not affect cell division (Fig. 3C, row 2), $MinC^{C}$ expression in conjunction with MinD can inhibit division. To ensure that the excess $MinC^{C}$ interacting with MinD was not responsible for inhibiting colony formation, a MinC mutant in which both domains have a lesion ($MinC^{G10D/R172A}$) was coexpressed with $MinC^{C}$. Coexpression of these MinCs along with MinD did not inhibit colony formation (Fig. 3C, row 6) indicating it is the heterodimer consisting of $MinC^{C}$ and $MinC^{R172A}$ that is responsible for inhibition. Western analysis indicated that $MinC^{R172A}$ and $MinC^{G10D/R172A}$, like $MinC^{R133A}$, are stable and expressed at 15 times the level of MinC (Fig. S5). Together, the above results directly challenge the notion that efficient inhibition of cell division depends on MinC/MinD copolymers *in vivo*.

MinC heterodimer deficient in copolymer formation is functional in spatial regulation

Based upon our findings (Fig. 2 and 3), copolymers of alternating MinC/MinD dimers are not necessary for the inhibitory activity of MinC/MinD. However, to test whether MinC/MinD copolymers are necessary for the spatial regulation of the Z ring we examined if they were necessary to prevent minicell formation and restore a wild type phenotype to a Δ*min* strain. Therefore, we reconstituted MinC heterodimers that are unable to polymerize in the context of the complete Min system using the same approach described in Fig. 3A and 3B to

determine whether MinC/MinD copolymer formation is essential for a wild type cell phenotype.

Expression of MinC^{R133A} alone did not significantly alter the phenotype of JS964 (Δ*min*) (Fig. 4, ii) as cells displayed heterogeneous lengths and minicells were present whereas expression of MinC/MinD/MinE from pSEB104CDE (P_{ara}::*minC minD minE*) complemented the Min phenotype and restored a wild type average cell length (Fig. 4, iii). Expression of MinC^{R133A} in conjunction with MinC/MinD/MinE in JS964 did not interfere with the ability of MinC/MinD/MinE to restore a wild type phenotype to the Δ*min* strain (Fig. 4, iv). Since the amount of MinC^{R133A} induced with 10 μM IPTG from pJF118EHC (P_{tac}::*minC*^{R133A}) is ~15-fold in excess of MinC induced with 0.2% arabinose (Fig. S1), most of the wild type MinC should be sequestered as heterodimers with MinC^{R133A} preventing copolymerization of MinC/MinD. To support this, we again tested the ability of two MinC mutants, both of which are inactive, to rescue MinC activity. JS964 with a plasmid pSEB104CDE-G10D (P_{ara}::*minC*^{G10D}*minD minE*) expressing MinC^{G10D}/MinD/MinE exhibited a Min$^-$ phenotype due to the impaired activity of the MinC^N domain (Fig. 4, v), however, coexpression of MinC^{R133A} restored a wild type phenotype with an average cell length the same as wild type (Fig. 4, vi and Fig. S6). The ability of MinC^{R133A} and MinC^{G10D} to complement and restore division inhibitory activity (Fig. 3B) as well as to rescue a Δ*min* phenotype (Fig. 4) indicates dimerization of the mutant proteins is occurring. This result again indicates that a MinC heterodimer, with one active MinC^N domain and one active MinC^C domain, even when present on opposite subunits, restores MinC activity.

MinC interaction with the FtsZ tail motif (conserved carboxy-terminal peptide)

The current model for MinC-dependent inhibition of Z ring formation posits that MinC activation by MinD involves recruitment of MinC to the membrane, which also augments MinC^C binding to the CCTP of FtsZ. This binding in turn positions MinC^N near an FtsZ polymer where it can contact the H10 helix of an FtsZ subunit once GTP is hydrolyzed (Shen & Lutkenhaus, 2010). It is not clear if MinD binding to MinC plays a direct role in MinC^C binding to the CCTP or more of an indirect role. Previous results, however, revealed that a MinD mutant unable to bind to the membrane can still augment the activity of MinC suggesting it increases the affinity of MinC for the Z ring and presumably the CCTP (Hu *et al.*, 2003).

We have already shown that a MinC heterodimer (MinC:MinC^{R133A}) that can only bind one MinD dimer appears as active as the wild type homodimer. Also, we observed that a heterodimer (MinC^{G10D}:MinC^{R133A}) formed by two inactive MinC mutants regained inhibitory activity, although to a lesser extent (Fig. 3B and S4A). This latter result indicates that MinD binding to one subunit of a dimer is sufficient to activate the other subunit. However, the dependency of the interaction with the CCTP upon MinD is not clear. If the CCTP interaction with MinC depends upon MinD then a CCTP would only bind to the wild type MinC (or MinC^{G10D}) subunit within the heterodimer. If, however, the binding is MinD independent then two CCTPs could bind per dimer, one to each of the MinC subunits. To assess this more directly we used a MinC mutant deficient in binding to the CCTP rather than a mutant deficient in binding MinD and therefore, polymerization.

MinC^{R172A} is unable to localize to septal rings in the presence of MinD and, although it oscillates in the presence of MinD/MinE, it fails to spatially regulate division. It also fails to localize to the Z ring when expressed with MinD in the absence of MinE (Zhou & Lutkenhaus, 2005). Expression of MinC^{R172A} along with MinC/MinD did not impair MinC/MinD activity (Fig. 5, row 3 vs row 4). Also, MinC^{R172A} can rescue MinC^{G10D} (Fig. 5A, row 6), although as with the MinC^{R133A}:MinC^{G10D} the MinC^{R172A}:MinC^{G10D} heterodimer was less active than a heterodimer with two active MinC^{N} domains. In this case the heterodimer can only bind one CCTP, i.e. the MinC^{G10D} subunit, which also binds MinD. Again it appears that CCTP binding to one subunit of the dimer is sufficient and, furthermore, it need not bind to the subunit with the active MinC^{N} domain. To make sure of this latter point a double MinC mutant was expressed along with MinC/MinD. Expression of MinC$^{G10D/R172A}$, carrying lesions in both domains, did not compromise the inhibition of colony formation (Fig. S4B, line 7 versus line 2) so it appears that a MinC heterodimer where MinD can bind to the subunit with the active MinC^{N} domain is as active as wild type MinC.

To further examine the mechanism of MinC activation by MinD, we tested the relationship between MinD and CCTP binding to MinC^{C} by uncoupling MinD from CCTP binding by reconstituting a MinC heterodimer composed of MinC^{R133A} and MinC^{R172A} *in vivo* (Fig. 1G). This heterodimer can still bind MinD through the MinC^{R172A} subunit. However, the MinC^{R172A} subunit can not bind the CCTP, and rescue of MinC activity would require that the MinC^{R133A} subunit still bind the CCTP in the absence of MinD binding. When MinC^{R172A} was expressed in JS964 (Δ*min*) along with MinC^{R133A}/MinD using 25 μM IPTG and 0.2% arabinose, respectively, cell viability was not affected (Fig. 5, line 8) and cells retained a typical minicell phenotype (data not shown). Together, these observations indicate that the CCTP of FtsZ interacts with the MinC^{C} subunit to which MinD is bound.

Activity of MinC in vitro

Ghosal *et al*. (Ghosal *et al.*, 2014) reported that MinC did not affect the assembly of FtsZ *in vitro* as assessed by sedimentation leading them to suggest a role for the MinC/MinD copolymer. This report is in contradiction to our previous finding that a MalE-MinC fusion blocked FtsZ sedimentation in a dose dependent manner (Hu *et al.*, 1999). We therefore reexamined the effect of MinC on FtsZ sedimentation. To do this analysis we used the MinC^{N} domain since the previous report indicated that this domain was responsible for the inhibitory activity (Hu & Lutkenhaus, 2000). Also, we used a His-tagged version of MinC^{N} instead of the MalE fusion used previously. As previously reported (Hu *et al.*, 1999, Hu & Lutkenhaus, 2000) MinC^{N} prevented the sedimentation of FtsZ in a dose dependent manner (Fig. 6). At a ratio of MinC^{N} to FtsZ of 0.5, MinC^{N} completely prevented FtsZ sedimentation. For a control we used the MinC^{G10D} mutant, which inactivates MinC^{N}. As expected, MinC$^{N\text{-}G10D}$ had little inhibitory activity, even when used at a 1:1 ratio. We conclude that MinC can prevent FtsZ sedimentation *in vitro*.

Discussion

It was recently proposed that activation of MinC by MinD involves formation of a new class of cytomotive filaments made of alternating dimers of MinC and MinD (Ghosal *et al.*, 2014). Although this model offers an explanation for why MinC is targeted to FtsZ filaments over FtsZ monomers, our results argue against a role for MinC/MinD copolymers in regulating Z ring assembly *in vivo*. Instead, our evidence favors a model in which the activation of MinC is mediated by a tripartite complex consisting of a dimer of MinC and a dimer of MinD bound to an FtsZ filament through a CCTP (Fig. 7). Furthermore, our results indicate that one MinD dimer is sufficient to recruit a MinC dimer to the membrane. Once at the membrane this MinC/MinD complex binds to the Z ring by interacting with a CCTP at a site formed at the interface of the MinC/MinD complex. We also find that one active $MinC^{N}$ domain in a heterodimer is sufficient but MinC is most efficient if this domain is on the same subunit that binds MinD.

MinD enhances the inhibitory activity of MinC about 25 to 50 fold (de Boer *et al.*, 1992). This activation can in part be accounted for by membrane localization and septal component targeting (Zhou & Lutkenhaus, 2005, Johnson *et al.*, 2002), however, it is possible that additional mechanisms exist. The cocrystallization of *A. aeolicus* $MinC^{C}$-MinD by Ghosal *et al.* (Ghosal *et al.*, 2014) suggested that MinC/MinD forms copolymers, which was supported by sedimentation and electron microscopy. They also observed these copolymers *in vivo* when MinC/MinD were overexpressed in the absence of MinE and suggested that the MinC/MinD copolymers were involved in the regulation of cytokinesis. In part, this possibility was raised by a failure to observe inhibition of FtsZ polymerization by MinC *in vitro.* Conti *et al.* (Conti *et al.*, 2015) also observed that MinC and MinD form stable polymers in the absence of lipid bilayers. Since they detected a linear filament with a MinD to MinC ratio 1.6:1, they probably observed the same type of filament reported by Ghosal *et al.*, even though they did not observe a critical concentration for assembly.

To test the copolymer model we sequestered $MinC^{WT}$ in a heterodimer by overexpression of a MinC mutant ($MinC^{R133A}$) deficient in MinD binding. Even though such a heterodimer is unable to form alternating copolymers with MinD, the cell division inhibitory activity of MinC was not diminished (Fig. 3A). This result indicates that MinC/MinD copolymerization is not required for suppressing cell division. This conclusion was supported and extended by the observation that coexpression of two MinC mutants, each with a lesion in a different domain of MinC, was able to rescue MinC activity. This rescue, along with bacterial 2-hybrid results, confirmed heterodimers were forming *in vivo* and indicated that a MinC heterodimer formed with a subunit with an active $MinC^{C}$ domain (can bind MinD and the CCTP) and another subunit with an active $MinC^{N}$ domain (can interact with FtsZ) is active, although somewhat less active than heterodimers in which one subunit has both of the active domains.

More convincing evidence that the copolymers are not involved in the regulation of the Z ring was obtained when $MinC^{R133A}$ was expressed in conjunction with $MinC^{G10D}$/MinD/MinE in a Δ*min* strain. Remarkably, the $MinC^{G10D}$/$MinC^{R133A}$ heterodimer was able to restore the wild type phenotype to a Δ*min* strain in the presence of MinD and MinE (Fig. 4).

Since MinD is in excess of MinC in vivo (7:1 ratio)(Szeto *et al.*, 2001, de Boer *et al.*, 1991, Li *et al.*, 2014), the most likely MinC/MinD complex would be a MinC heterodimer bound to a MinD dimer.

Consistent with the results obtained with MinC mutants, when wild type MinD was forced to form a heterodimer by over expression of a MinD mutant ($MinD^{D154A}$) deficient in MinC binding, which would abrogate MinC/MinD copolymerization, the MinC-mediated suppression of cell division was not attenuated (Fig. 2A). Since the $MinD^{WT/D154A}$ heterodimer retains an intact dimeric surface available for MinC binding, trimers consisting of a MinC dimer bridging two MinD heterodimer may form. In this case, the high ratio of MinD to MinC *in vivo* (7:1) favors such a tripartite complex. However, based on our studies with MinC heterodimer, such a tripartite complex might not be necessary for MinC activation by MinD. The dominant negative phenotype of $MinD^{T91K/D154A}$ confirmed MinD heterodimers ($MinD^{WT}$/$MinD^{T91K/D154A}$) were forming *in vivo* (Fig. 2A).]

Intriguingly, the $MinC^{R133A/R172A}$ heterodimer was unable to suppress cell division in the presence of MinD. Since MinD can only interact with the $MinC^{R172A}$ subunit and the CCTP only has the potential to interact with the $MinC^{R133A}$ subunit, the failure to reconstitute MinC activity leads us to conclude that CCTP binding to $MinC^{C}$ requires MinD be bound to that domain. Either it binds to at an interface formed when MinD binds to $MinC^{C}$ or MinD binding to the ^{133}RSGQ^{136} induces a conformational change that increases the affinity for CCTP. Both are possible as the ^{133}RSGQ^{136} motif is close to the R^{172} residue (~ 1 nm) on MinC. We favor the former as MinD binding appears to induce little conformational change in MinC (Ghosal *et al.*, 2014).

The genetic evidence shows convincingly that copolymers of MinC/MinD are not required for spatial regulation of the Z ring. Also, arguing against the copolymer model is the ratio of MinD to MinC which is estimated to be ~7:1 *in vivo* under different growth conditions (Li *et al.*, 2014); less than 15% of the MinD population would be bound by MinC to constitute the inhibitory MinC/MinD complex. In this situation, it is more likely that the MinC dimers dispersed in the MinD polar zone are sufficient to prevent polar Z ring formation. A nonpolymeric MinC/MinD complex at the membrane likely attaches to an FtsZ filament by binding an unoccuppied CCTP (Fig. 7). This brings the $MinC^{N}$ domain to the FtsZ filament, which leads to fragmentation of the filament as previously proposed (Shen & Lutkenhaus, 2010). This mode of action is advantageous, since a few MinC/MinD complexes acting independent of each other may sufficiently fragment FtsZ filaments to prevent their assembly into the Z ring. The observation that MinC heterodimers that are as active as wild type MinC have MinD bound to the same subunit with the active $MinC^{N}$ indicates MinD may activate $MinC^{N}$ by restricting its motion or enhancing its orientation.

Some results indicated that the MinCDE proteins were organized into extended coiled structures winding around the cell between the poles (Shih *et al.*, 2003). Although the coiled structures of the Min proteins are likely to be microscopic artifacts, it is noteworthy that distribution pattern of MinC was almost identical to that of MinD in those studies. In previous observations of GFP-MinC, MinC dynamics closely resembles MinD oscillation (Hu & Lutkenhaus, 1999, Raskin & de Boer, 1999), supporting our idea that MinC is well

dispersed with MinD *in vivo*. It is well documented that overproduction of MinC in a wild type strain leads to Z ring destruction and inhibition of division (Geissler *et al.*, 2003). Possibly under these conditions MinC/MinD copolymers form and interfere with the oscillation. Also, MinC competing with MinE likely disrupts the oscillation which may be sufficient to cause division inhibition by redistributing MinC/MinD away from polar zones. Consistent with this, Min reconstitution experiments *in vitro* demonstrated that increasing the level of MinC interferes with the Min oscillation (Loose *et al.*, 2011).

Our *in vitro* studies using sedimentation confirmed that MinC/MinD copolymers can form *in vitro* as previously reported (Ghosal *et al.*, 2014, Conti *et al.*, 2015). We also demonstrated that $MinD^{D154A}$, which is unable to bind MinC, can prevent MinC/MinD copolymer formation *in vitro* when added in excess consistent with heterodimer formation (Fig. 2B). This prevention of copolymer formation *in vitro* along with the failure of $MinD^{D154A}$ to disrupt the inhibitory activity of MinC/MinD *in vivo* is consistent with our conclusion that MinC/MinD copolymers are not needed for MinC/MinD inhibitory activity *in vivo*.

Previously, we observed that MinC prevented FtsZ sedimentation *in vitro* and that this activity could be attributed to $MinC^{N}$ (Hu *et al.*, 1999; Hu & Lutkenhaus, 2000). Here we confirmed that $MinC^{N}$ prevented FtsZ sedimentation in dosage dependent manner with a 0.5:1 ratio of $MinC^{N}$ to FtsZ leading to a complete block. This ability of MinC to prevent FtsZ sedimentation is consistent with the observation that MinC shortens FtsZ polymers *in vitro* (Dajkovic *et al.*, 2008, Hernandez-Rocamora *et al.*, 2013) and can disassemble an FtsZ filament network attached to a membrane support even without MinD (Arumugam *et al.*, 2014). The high level of MinC needed *in vitro* compared to the *in vivo* ratio of MinC to FtsZ (0.1 to 1) (Li *et al.*, 2014) indicates that the *in vitro* reaction does not fully capture the *in vivo* mode of action of MinC/MinD. However, this *in vitro* inhibitory activity is prevented by the $minC^{G10D}$ mutation, indicating that this activity is likely to be relevant *in vivo*.

While we were investigating the validity of the MinCD copolymerization model we uncovered clues to the mechanistic underpinning of MinC activation by MinD. MinD's interaction with the RSGQ motif on the $MinC^{C}$ surface likely generates a binding site for the CCTP of FtsZ (Fig. 7) positioning the MinC/MinD complex near the FtsZ filament. A MinC/MinD complex on the inner surface of the cytoplasmic membrane is analogous to ZipA or FtsA in terms of its ability to capture a CCTP. In this model membrane bound proteins like ZipA, FtsA and MinC/MinD that have weak affinity for the CCTP of FtsZ combine to generate high avidity for an FtsZ filament without themselves having to polymerize. The avidity favors such proteins binding an FtsZ filament over a monomer by 50 fold (Du *et al.*, 2015).

One question that arises from this study is why MinC is dimeric? MinD and MinE are also dimeric but for these proteins the reasons appear obvious. MinD uses ATPase hydrolysis to cycle between dimeric and monomeric states, which have different affinities for the membrane and its partners (Lackner *et al.*, 2003, Wu *et al.*, 2011, Hu *et al.*, 2003). In contrast, MinE is always a dimer but cycles between two conformations: an active form that binds MinD and the membrane and a latent form that diffuses in the cytoplasm (Park *et al.*, 2011, Ghasriani *et al.*, 2010, Ramos *et al.*, 2006, Kang *et al.*, 2010). The dimeric nature of

MinE facilitates this interconversion and the ability of MinE to linger on the membrane. MinC is always a dimer (Cordell *et al.*, 2001, Szeto *et al.*, 2001, Hu & Lutkenhaus, 2000, Arumugam *et al.*, 2014), as well, and is therefore suited to bridge two MinD dimers resulting in an alternating copolymer of MinC/MinD dimers. However, our genetic analysis demonstrating that heterodimers between MinC or MinD mutants and the wild type protein are functional even though they are unable to form copolymers indicates this is not the role of the MinC dimer.

Experimental Procedures

Strains and media

The *E. coli* K-12 strain JS964 (*MC1061 malP::lacI*^{q} *minB::Kan*) was primarily used in this study. *E.coli* FtsZ was expressed in JS238 (JS219 *srlC::Tn10 recA1*) for purification. For western blot to detect endogenous MinC protein, JS219 strain (MC1061 *malP::lacI*^{q}) was used. For MinC$^{1–115}$ expression and purification, BL21 (λDE3) strain (*F*$^{–}$ *ompT gal dcm lon hsdS*$_{B}$*(r*$_{B}^{-}$*m*$_{B}^{-}$*) λ(DE3 [lacI lacUV5-T7 gene 1 ind1 sam7 nin5]*) was used. Plasmid construction and other protein purifications were carried out using JS964 strain grown at 37°C. LB (Luria-Bertani) medium containing 0.5% NaCl was used and antibiotics (ampicillin 100 μg/ml, spectinomycin 50 μg/ml), IPTG, glucose (0.2%), and arabinose (0.2%) were added as indicated. Bacterial 2-hybrid test was done with strain BTH101 (Δ*min*) as previously described (Park *et al.*, 2012).

Microscopy

Plasmid pJF118EHC^{R133A} (P*tac::minC*^{R133A}) were transformed with pSEB104CDE (P*ara::minC minD minE*) or its derivative pSEB104C^{G10D}DE (P*ara::minC*^{G10D} *minD minE*) into JS964 strain (Δ*min*). Single colonies were inoculated into LB containing ampicillin, spectinomycin, 0.2% arabinose, and 10 μM IPTG and cultured overnight at 37°C. Next day, each culture was further diluted 1000-fold and grown until mid-log phase under the condition described above. Cells were directly taken from exponential cultures and mounted onto an agarose pad that contained 1% agarose and 50% LB. Cellular phenotypes were examined by phase-contrast microscopy and images were recorded with CoolSNAP HQ2 CCD camera. Cell length measurements (over 200 per each sample) were made with Metamorph software (Molecular Devices). One-way analysis of variance (Bonferroni method) was used for statistical analysis using Graphpad Prism (Graphpad software, Inc).

Plasmids

To construct plasmid pJF118EHC (P*tac::minC*), *E. coli* minC ORF was PCR amplified using pSEB104CD as a template and digested with BamHI/HindIII prior to ligation into BamHI/HindIII-digested pJF118EH vector. Plasmid pSEB104CD (Para::*minC minD*), pJB216 (Plac::*minE*), and pZH115 (Ptac::minD) were previously described (Hu *et al.*, 2002). To create pSEB104CDE (Para::*minC minD minE*), BstXI/HindIII fragment from pJPB210 was excised and *ligated* into pSEB104CD that was linearized with BstXI/HindIII. For construction of pET21α-MinC$^{1–115}$, pSEB104CD was used for a PCR template to obtain the *E.coli minC*$^{1–115}$ fragment that was subsequently digested with NdeI/XhoI and cloned into pET21α (Novagen). Plasmids pBang55 and pSEB160 were previously detailed

(Du & Lutkenhaus, 2014, Shen & Lutkenhaus, 2011). Plasmids used for bacterial 2-hybrid tests were pCT25-MinC, pUT18-MinC and pCT25-MinD (Zhou & Lutkenhaus, 2005; Park *et al.*, 2012).

Protein expression and purification

For $MinC^{1–115}$-6xHis purification, IPTG (1mM) was added to 1L culture of BL21 (λDE3)/ pET21α-$MinC^{115}$ at OD_{540}~0.5 and incubated for 2–3 hours. Cells were harvested by centrifugation and resuspended in lysis buffer (25 mM Tris-HCl [pH7.9], 100 mM NaCl, 10 mM Imidazole, 10% Glycerol, 500 μM DTT) and lysed with a French press. Cell debris was removed by centrifugation at 10,000xg at 4 °C for 30 min and the supernatant was collected and applied to nickel-agarose column that was pre-equilibrated with the lysis buffer. The column was washed with a washing buffer (25 mM Tris-HCl [pH7.9], 500 mM NaCl, 20 mM imidazole, 0.1% NP-40) and then a second washing buffer (25 mM Tris-HCl [pH7.9], 500 mM NaCl, 50 mM imidazole). The protein was eluted with elution buffer (25 mM Tris-HCl [pH7.9], 500 mM NaCl, 250 mM imidazole). The peak fractions were pooled together, and dialyzed against 1 liter of dialysis buffer (25 mM HEPES-NaOH [pH 6.8], 50 mM KCl, 1mM DTT) and concentrated to obtain a desirable concentration using a centrifugal filter (Amicon Ultra). For purification of *E.coli* FtsZ, arabinose (0.2%) was added to 1L culture of JS238 strain/pSEB160 and incubated for 3 hours. Cells were collected by centrifugation and the pellets were resuspended in Buffer A (50 mM Tris-HCl [pH7.9], 50 mM NaCl, 10% glycerol, 0.5mM EDTA) and subjected to a French press. Cell lysates were sequentially centrifuged at 10,000xg and 20, 000xg for 30 min and 50 min, respectively. FtsZ protein was selectively precipitated using 30% ammonium sulfate. The precipitated pellets were resuspended, dialyzed overnight in Buffer A and loaded onto ResQ anion exchange column coupled to FPLC system (GE Healthcare) and eluted with a gradient of NaCl (50–500 mM) in Buffer A. Peak fractions of FtsZ were pooled, concentrated, and dialyzed in Buffer B (25 mM HEPES-NaOH [pH7.2], 10% glycerol, 100 μM EDTA). The procedures for purification of full length MinD, MinE-6xHIS and MalE-$MinC^{116–231}$ were previously described (Park *et al.*, 2011, Park *et al.*, 2012, Hu & Lutkenhaus, 2000).

MinC/MinD binding to MLVs

Preparation of multilamellar vesicles (MLVs) was previously described (Park *et al.*, 2012). MinD (5 μM) or $MinD^{D154A}$ (5 μM) were incubated with MLVs (400 ng/μl) in 1xATPase buffer (25 mM Tris-HCl [pH7.5], 50 mM KCl, 5 mM $MgCl_2$). MalE-$MinC^{C}$ (5 μM) along with ADP or ATP (1 mM). MinE-6xHIS (5 μM) was added to the reactions that contain $MinD^{D154A}$ and MalE-$MinC^{C}$. The samples are incubated at 25°C for 10 min and centrifuged at 16,800xg for 5 min. Collected pellets and supernatants were analyzed on 12% polyacrylamide gel electrophoresis (PAGE).

Site-directed mutagenesis

Various *minC* mutations such as $minC^{G10D}$, $minC^{R133A}$, and $minC^{R172A}$ were introduced into *minC* on pJF118EHC, pSEB104CD, pSEB104CDE, pCT25-MinC and pUT18-MinC using a QuickChange II site-directed mutagenesis kit according to manufacturer's

instruction (Agilent Technologies). *minD* mutations such as *minD*^{T91K} and *minD*^{D154A} were introduced into *minD* on pZH115 using the same method.

Sedimentation assays

To assess MinC/MinD copolymerization, MinD (5 μM) and MBP-MinC^{C} (5 μM) were incubated in 1xPol buffer (25mM MES-NaOH [pH 6.5], 50 mM KCl, 10 mM $MgCl_2$) in the presence of ADP or ATP (4 mM) for 10 min at 25°C. The reaction mixtures were centrifuged at 175,000xg for 15 min in TLA 100.2 rotor (Beckman). Pellets and supernatants were analyzed on 12.5 % PAGE and with Coomassie blue staining. To reconstitute MinD^{WT}/MinD^{D154A} heterodimer that prevents MinC/MinD copolymerization, MinD^{D154A} (10 μM) was added to the afore-described reactions that contain ADP or ATP (4 mM). To examine MinC-dependent prevention of FtsZ polymerization, FtsZ (5 μM) and increasing concentrations of MinC^{115}-6xHIS (0–5 μM) were incubated in 1xPol buffer (25 mM MES-NaOH [pH 6.8], 50 mM KCl, 10 mM $MgCl_2$) at 25°C for 5 min in the presence of GDP or GTP (2 mM). In a control reaction MinC^{N}-G10D was added at 5 μM. The reactions were centrifuged as described above and collected pellets were analyzed on 12.5% PAGE and with Coomassie blue staining.

Western blot

JS219, a wild-type strain, containing pJF118EH and pGB2 vectors, and JS964 (Δ*min*) containing pJF118EH or derivatives expressing *minC* alleles in combination with pGB2 or pSEB104CDE were grown in LB medium overnight in the presence of ampicillin and spectinomycin. The next day cells were diluted 1000-fold and cultured to optical density 0.1 prior to prior to induction with 0.2% arabinose and 10 μM IPTG for 2 hr. Cells were collected by centrifugation at 14,500 × g for 1min, diluted with sterile water, resuspended in SDS sample buffer, and boiled for 5 min. Samples were subjected to SDS-polyacrylamide gel electrophoresis, transferred to a nitrocellulose membrane, and blocked overnight with PBS containing 5% milk. A rabbit antiserum raised against 6X-His-MinC was used for primary antibody and goat alkaline phosphatase-conjugated anti-rabbit secondary antibody was used for MinC detection.

Supplementary Material

Refer to Web version on PubMed Central for supplementary material.

Acknowledgments

This work was supported by NIH grant GM29764.

References

Arumugam S, Petrasek Z, Schwille P. MinCDE exploits the dynamic nature of FtsZ filaments for its spatial regulation. Proceedings of the National Academy of Sciences of the United States of America. 2014; 111:E1192–1200. [PubMed: 24707052]

Bernhardt TG, de Boer PA. SlmA, a nucleoid-associated, FtsZ binding protein required for blocking septal ring assembly over Chromosomes in E. coli. Molecular cell. 2005; 18:555–564. [PubMed: 15916962]

Bi EF, Lutkenhaus J. FtsZ ring structure associated with division in Escherichia coli. Nature. 1991; 354:161–164. [PubMed: 1944597]

Conti J, Viola MG, Camberg JL. The bacterial cell division regulators MinD and MinC form polymers in the presence of nucleotide. FEBS letters. 2015; 589:201–206. [PubMed: 25497011]

Cordell SC, Anderson RE, Lowe J. Crystal structure of the bacterial cell division inhibitor MinC. The EMBO journal. 2001; 20:2454–2461. [PubMed: 11350934]

Dajkovic A, Lan G, Sun SX, Wirtz D, Lutkenhaus J. MinC spatially controls bacterial cytokinesis by antagonizing the scaffolding function of FtsZ. Current biology: CB. 2008; 18:235–244. [PubMed: 18291654]

de Boer PA. Advances in understanding E. coli cell fission. Current opinion in microbiology. 2010; 13:730–737. [PubMed: 20943430]

de Boer PA, Crossley RE, Hand AR, Rothfield LI. The MinD protein is a membrane ATPase required for the correct placement of the Escherichia coli division site. The EMBO journal. 1991; 10:4371–4380. [PubMed: 1836760]

de Boer PA, Crossley RE, Rothfield LI. A division inhibitor and a topological specificity factor coded for by the minicell locus determine proper placement of the division septum in E. coli. Cell. 1989; 56:641–649. [PubMed: 2645057]

de Boer PA, Crossley RE, Rothfield LI. Roles of MinC and MinD in the site-specific septation block mediated by the MinCDE system of Escherichia coli. Journal of bacteriology. 1992; 174:63–70. [PubMed: 1729224]

Du S, Lutkenhaus J. SlmA antagonism of FtsZ assembly employs a two-pronged mechanism like MinCD. PLoS genetics. 2014; 10:e1004460. [PubMed: 25078077]

Du S, Park KT, Lutkenhaus J. Oligomerization of FtsZ converts the FtsZ tail motif conserved carboxy-terminal peptide into a multivalent ligand with high avidity for partners ZipA and SlmA. Molecular microbiology. 2015; 95:173–188. [PubMed: 25382687]

Ebersbach G, Gerdes K. Bacterial mitosis: partitioning protein ParA oscillates in spiral-shaped structures and positions plasmids at mid-cell. Molecular microbiology. 2004; 52:385–398. [PubMed: 15066028]

Ebersbach G, Gerdes K. Plasmid segregation mechanisms. Annual review of genetics. 2005; 39:453–479.

Geissler B, Elraheb D, Margolin W. A gain-of-function mutation in ftsA bypasses the requirement for the essential cell division gene zipA in Escherichia coli. Proceedings of the National Academy of Sciences of the United States of America. 2003; 100:4197–4202. [PubMed: 12634424]

Ghasriani H, Ducat T, Hart CT, Hafizi F, Chang N, Al-Baldawi A, Ayed SH, Lundstrom P, Dillon JA, Goto NK. Appropriation of the MinD protein-interaction motif by the dimeric interface of the bacterial cell division regulator MinE. Proceedings of the National Academy of Sciences of the United States of America. 2010; 107:18416–18421. [PubMed: 20937912]

Ghosal D, Trambaiolo D, Amos LA, Lowe J. MinCD cell division proteins form alternating copolymeric cytomotive filaments. Nature communications. 2014; 5:5341.

Gitai Z. Plasmid segregation: a new class of cytoskeletal proteins emerges. Current biology: CB. 2006; 16:R133–136. [PubMed: 16488865]

Hernandez-Rocamora VM, Garcia-Montanes C, Reija B, Monterroso B, Margolin W, Alfonso C, Zorrilla S, Rivas G. MinC protein shortens FtsZ protofilaments by preferentially interacting with GDP-bound subunits. The Journal of biological chemistry. 2013; 288:24625–24635. [PubMed: 23853099]

Hu Z, Gogol EP, Lutkenhaus J. Dynamic assembly of MinD on phospholipid vesicles regulated by ATP and MinE. Proceedings of the National Academy of Sciences of the United States of America. 2002; 99:6761–6766. [PubMed: 11983867]

Hu Z, Lutkenhaus J. Topological regulation of cell division in Escherichia coli involves rapid pole to pole oscillation of the division inhibitor MinC under the control of MinD and MinE. Molecular microbiology. 1999; 34:82–90. [PubMed: 10540287]

Hu Z, Lutkenhaus J. Analysis of MinC reveals two independent domains involved in interaction with MinD and FtsZ. Journal of bacteriology. 2000; 182:3965–3971. [PubMed: 10869074]

Hu Z, Lutkenhaus J. Topological regulation of cell division in E. coli. spatiotemporal oscillation of MinD requires stimulation of its ATPase by MinE and phospholipid. Molecular cell. 2001; 7:1337–1343. [PubMed: 11430835]

Hu Z, Lutkenhaus J. A conserved sequence at the C-terminus of MinD is required for binding to the membrane and targeting MinC to the septum. Molecular microbiology. 2003; 47:345–355. [PubMed: 12519187]

Hu Z, Mukherjee A, Pichoff S, Lutkenhaus J. The MinC component of the division site selection system in Escherichia coli interacts with FtsZ to prevent polymerization. Proceedings of the National Academy of Sciences of the United States of America. 1999; 96:14819–14824. [PubMed: 10611296]

Hu Z, Saez C, Lutkenhaus J. Recruitment of MinC, an inhibitor of Z-ring formation, to the membrane in Escherichia coli: role of MinD and MinE. Journal of bacteriology. 2003; 185:196–203. [PubMed: 12486056]

Ivanov V, Mizuuchi K. Multiple modes of interconverting dynamic pattern formation by bacterial cell division proteins. Proceedings of the National Academy of Sciences of the United States of America. 2010; 107:8071–8078. [PubMed: 20212106]

Johnson JE, Lackner LL, de Boer PA. Targeting of DMinC/MinD and DMinC/DicB complexes to septal rings in Escherichia coli suggests a multistep mechanism for MinC-mediated destruction of nascent FtsZ rings. Journal of bacteriology. 2002; 184:2951–2962. [PubMed: 12003935]

Johnson JE, Lackner LL, Hale CA, de Boer PA. ZipA is required for targeting of DMinC/DicB, but not DMinC/MinD, complexes to septal ring assemblies in Escherichia coli. Journal of bacteriology. 2004; 186:2418–2429. [PubMed: 15060045]

Kang GB, Song HE, Kim MK, Youn HS, Lee JG, An JY, Chun JS, Jeon H, Eom SH. Crystal structure of Helicobacter pylori MinE, a cell division topological specificity factor. Molecular microbiology. 2010; 76:1222–1231. [PubMed: 20398219]

Lackner LL, Raskin DM, de Boer PA. ATP-dependent interactions between Escherichia coli Min proteins and the phospholipid membrane in vitro. Journal of bacteriology. 2003; 185:735–749. [PubMed: 12533449]

Leonard TA, Butler PJ, Lowe J. Bacterial chromosome segregation: structure and DNA binding of the Soj dimer--a conserved biological switch. The EMBO journal. 2005; 24:270–282. [PubMed: 15635448]

Li GW, Burkhardt D, Gross C, Weissman JS. Quantifying absolute protein synthesis rates reveals principles underlying allocation of cellular resources. Cell. 2014; 157:624–635. [PubMed: 24766808]

Loose M, Fischer-Friedrich E, Herold C, Kruse K, Schwille P. Min protein patterns emerge from rapid rebinding and membrane interaction of MinE. Nature structural & molecular biology. 2011; 18:577–583.

Lowe J, Amos LA. Evolution of cytomotive filaments: the cytoskeleton from prokaryotes to eukaryotes. The international journal of biochemistry & cell biology. 2009; 41:323–329. [PubMed: 18768164]

Lutkenhaus J. Assembly dynamics of the bacterial MinCDE system and spatial regulation of the Z ring. Annual review of biochemistry. 2007; 76:539–562.

Lutkenhaus J. The ParA/MinD family puts things in their place. Trends in microbiology. 2012; 20:411–418. [PubMed: 22672910]

Lutkenhaus J, Pichoff S, Du S. Bacterial cytokinesis: From Z ring to divisome. Cytoskeleton. 2012; 69:778–790. [PubMed: 22888013]

Lutkenhaus J, Sundaramoorthy M. MinD and role of the deviant Walker A motif, dimerization and membrane binding in oscillation. Molecular microbiology. 2003; 48:295–303. [PubMed: 12675792]

Ma L, King GF, Rothfield L. Positioning of the MinE binding site on the MinD surface suggests a plausible mechanism for activation of the Escherichia coli MinD ATPase during division site selection. Molecular microbiology. 2004; 54:99–108. [PubMed: 15458408]

Margolin W. FtsZ and the division of prokaryotic cells and organelles. Nature reviews Molecular cell biology. 2005; 6:862–871. [PubMed: 16227976]

Meinhardt H, de Boer PA. Pattern formation in Escherichia coli: a model for the pole-to-pole oscillations of Min proteins and the localization of the division site. Proceedings of the National Academy of Sciences of the United States of America. 2001; 98:14202–14207. [PubMed: 11734639]

Park KT, Wu W, Battaile KP, Lovell S, Holyoak T, Lutkenhaus J. The Min oscillator uses MinD-dependent conformational changes in MinE to spatially regulate cytokinesis. Cell. 2011; 146:396–407. [PubMed: 21816275]

Park KT, Wu W, Lovell S, Lutkenhaus J. Mechanism of the asymmetric activation of the MinD ATPase by MinE. Molecular microbiology. 2012; 85:271–281. [PubMed: 22651575]

Ramirez-Arcos S, Greco V, Douglas H, Tessier D, Fan D, Szeto J, Wang J, Dillon JR. Conserved glycines in the C terminus of MinC proteins are implicated in their functionality as cell division inhibitors. Journal of bacteriology. 2004; 186:2841–2855. [PubMed: 15090526]

Ramos D, Ducat T, Cheng J, Eng NF, Dillon JA, Goto NK. Conformation of the cell division regulator MinE: evidence for interactions between the topological specificity and anti-MinCD domains. Biochemistry. 2006; 45:4593–4601. [PubMed: 16584194]

Raskin DM, de Boer PA. MinDE-dependent pole-to-pole oscillation of division inhibitor MinC in Escherichia coli. Journal of bacteriology. 1999; 181:6419–6424. [PubMed: 10515933]

Sen M, Rothfield LI. Stability of the Escherichia coli division inhibitor protein MinC requires determinants in the carboxy-terminal region of the protein. Journal of bacteriology. 1998; 180:175–177. [PubMed: 9422610]

Shen B, Lutkenhaus J. The conserved C-terminal tail of FtsZ is required for the septal localization and division inhibitory activity of MinCC/MinD. Molecular microbiology. 2009; 72:410–424. [PubMed: 19415799]

Shen B, Lutkenhaus J. Examination of the interaction between FtsZ and MinCN in E. coli suggests how MinC disrupts Z rings. Molecular microbiology. 2010; 75:1285–1298. [PubMed: 20132438]

Shen B, Lutkenhaus J. Differences in MinC/MinD sensitivity between polar and internal Z rings in Escherichia coli. Journal of bacteriology. 2011; 193:367–376. [PubMed: 21097625]

Shih YL, Le T, Rothfield L. Division site selection in Escherichia coli involves dynamic redistribution of Min proteins within coiled structures that extend between the two cell poles. Proceedings of the National Academy of Sciences of the United States of America. 2003; 100:7865–7870. [PubMed: 12766229]

Shih YL, Rothfield L. The bacterial cytoskeleton. Microbiology and molecular biology reviews: MMBR. 2006; 70:729–754. [PubMed: 16959967]

Shiomi D, Margolin W. The C-terminal domain of MinC inhibits assembly of the Z ring in Escherichia coli. Journal of bacteriology. 2007; 189:236–243. [PubMed: 17085577]

Suefuji K, Valluzzi R, RayChaudhuri D. Dynamic assembly of MinD into filament bundles modulated by ATP, phospholipids, and MinE. Proceedings of the National Academy of Sciences of the United States of America. 2002; 99:16776–16781. [PubMed: 12482939]

Szardenings F, Guymer D, Gerdes K. ParA ATPases can move and position DNA and subcellular structures. Current opinion in microbiology. 2011; 14:712–718. [PubMed: 21963112]

Szeto TH, Rowland SL, King GF. The dimerization function of MinC resides in a structurally autonomous C-terminal domain. Journal of bacteriology. 2001; 183:6684–6687. [PubMed: 11673440]

Tonthat NK, Arold ST, Pickering BF, Van Dyke MW, Liang S, Lu Y, Beuria TK, Margolin W, Schumacher MA. Molecular mechanism by which the nucleoid occlusion factor, SlmA, keeps cytokinesis in check. The EMBO journal. 2011; 30:154–164. [PubMed: 21113127]

Vecchiarelli AG, Mizuuchi K, Funnell BE. Surfing biological surfaces: exploiting the nucleoid for partition and transport in bacteria. Molecular microbiology. 2012; 86:513–523. [PubMed: 22934804]

Wu LJ, Errington J. Coordination of cell division and chromosome segregation by a nucleoid occlusion protein in Bacillus subtilis. Cell. 2004; 117:915–925. [PubMed: 15210112]

Wu W, Park KT, Holyoak T, Lutkenhaus J. Determination of the structure of the MinD-ATP complex reveals the orientation of MinD on the membrane and the relative location of the binding sites for MinE and MinC. Molecular microbiology. 2011; 79:1515–1528. [PubMed: 21231967]

Zhou H, Lutkenhaus J. MinC mutants deficient in MinD- and DicB-mediated cell division inhibition due to loss of interaction with MinD, DicB, or a septal component. Journal of bacteriology. 2005; 187:2846–2857. [PubMed: 15805531]

Zhou H, Schulze R, Cox S, Saez C, Hu Z, Lutkenhaus J. Analysis of MinD mutations reveals residues required for MinE stimulation of the MinD ATPase and residues required for MinC interaction. Journal of bacteriology. 2005; 187:629–638. [PubMed: 15629934]

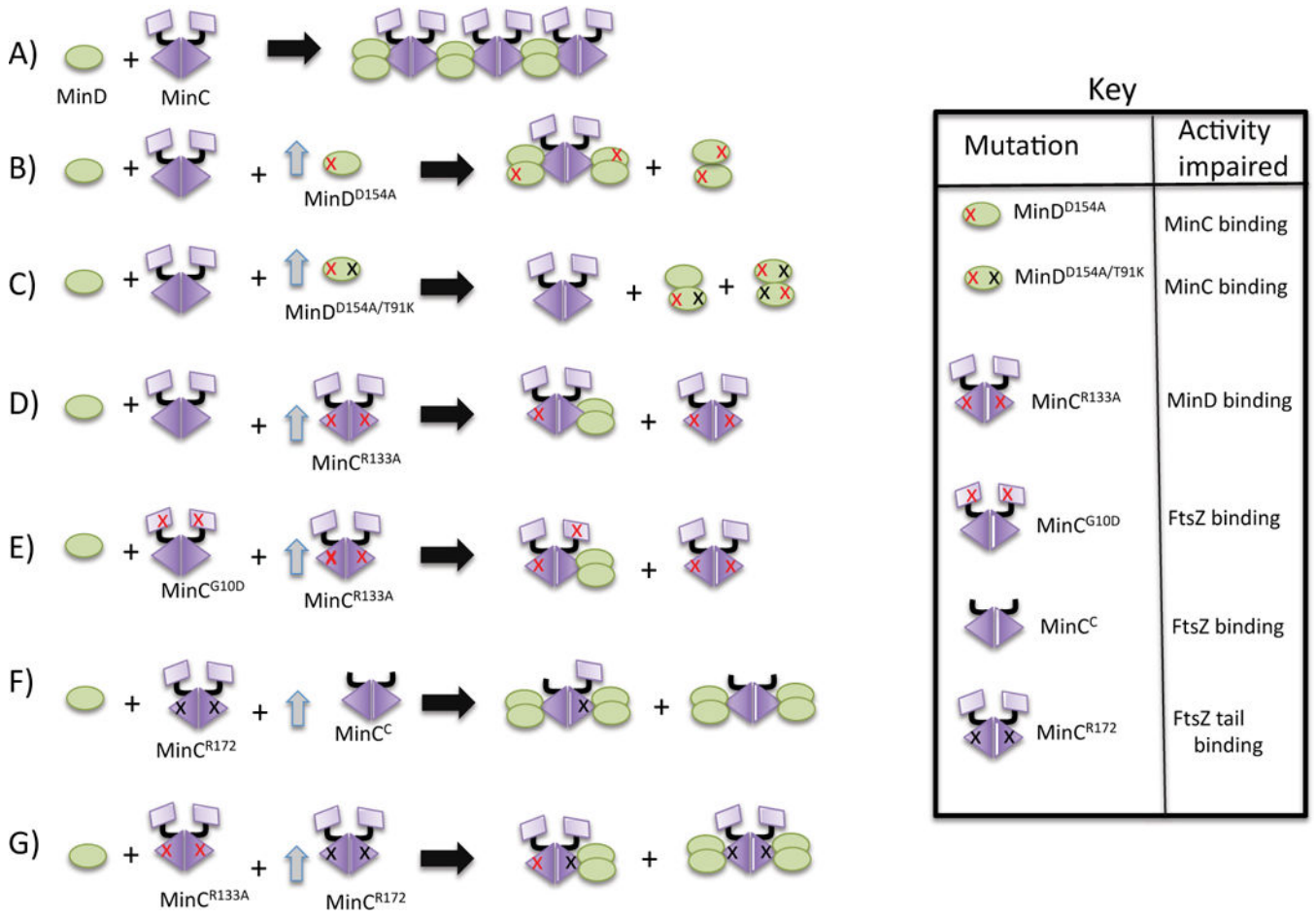

Fig. 1.

Strategy employed to test the physiological role of MinC/MinD copolymers. A) Due to symmetry and the location of binding sites MinC and MinD can make a copolymer of alternating dimers. B) Overexpression of $MinD^{D154A}$ in the presence of WT MinD/MinC results in heterodimer that can bind MinC on only one side. Such a heterodimer can not form alternating copolymers. The excess $MinD^{D154A}$ is relatively nontoxic as it does not bind MinC. C) Overexpression of $MinD^{D154A/T92K}$ in the presence of WT MinD/MinC leads to heterodimer formation with WT MinD. Such a heterodimer is unable to bind MinC as both binding sites are inactivated. The heterodimer should inactivate MinD. D) Excess expression of $MinC^{R133A}$ in a strain expressing WT MinC/MinD leads to formation of MinC:$MinC^{R133A}$ heterodimers, which can only bind MinD on one side of the heterodimer. The $MinC^{R133A}$ in excess of the wild type MinC forms homodimers that are relatively less toxic because they can not bind MinD. E) Excess expression of $MinC^{R133A}$ in a strain expressing $MinC^{G10D}$ also results in a heterodimer that can only bind MinD on one side of the MinC. Note MinD binds to the MinC subunit with an inactive $MinC^{N}$. F). Overexpression of $MinC^{C}$ in the presence of $MinC^{R172A}$/MinD. G) Excess expression of $MinC^{R172A}$ with $MinC^{R133A}$ leads to a heterodimer in which the $MinC^{C}$ domains have different defects. In this case MinD can bind to the $MinC^{R172A}$ subunit but the CCTP of FtsZ can not bind to this subunit.

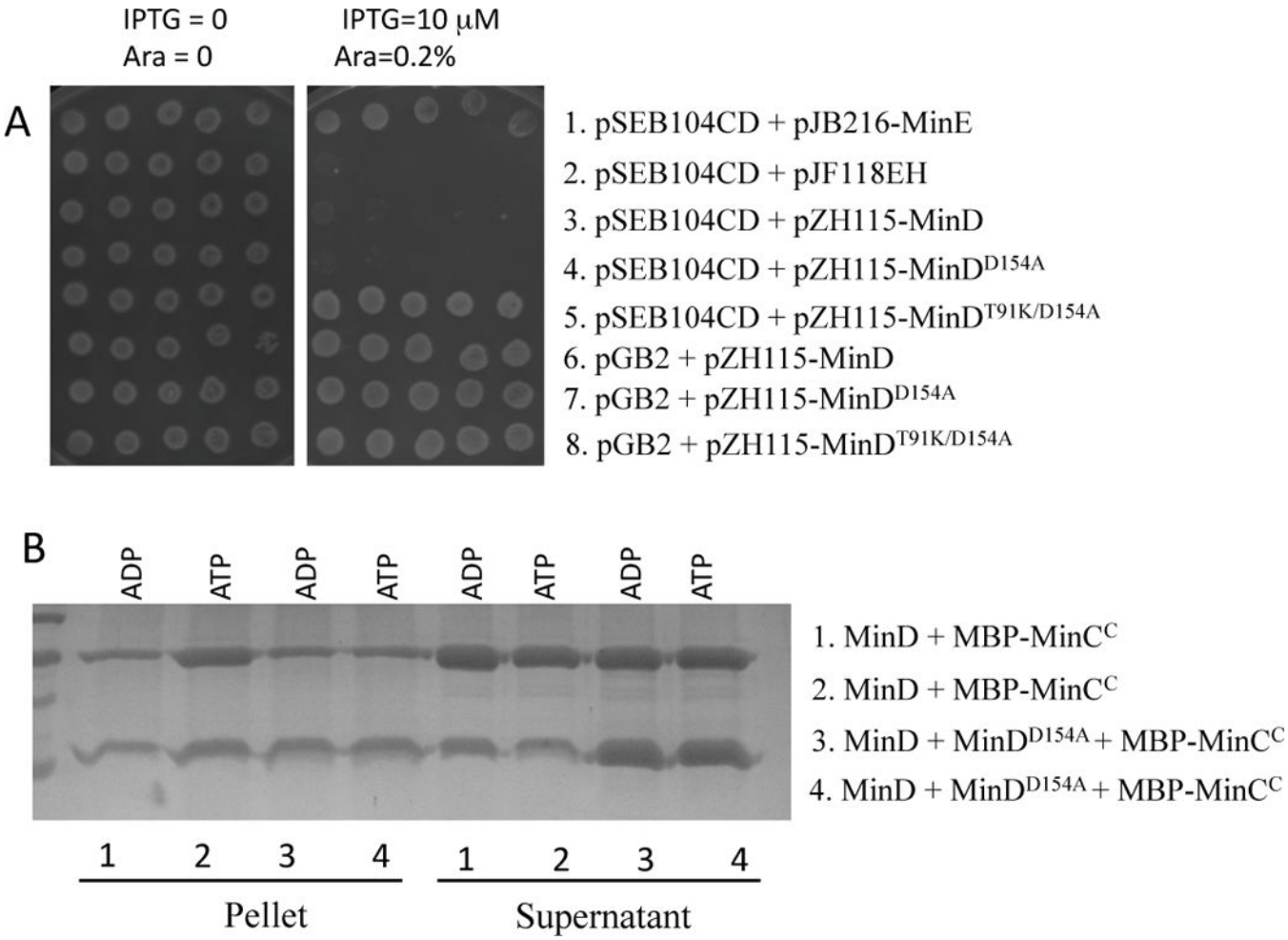

Fig. 2.

Effect of MinD heterodimer formation on MinC/MinD activity *in vivo* and MinC/MinD copolymerization *in vitro*. A) pZH115 (P_{tac}::*minD*) and derivatives of this plasmid containing the *minD*^{D154A} and *minD*$^{T91K/D154A}$ mutations were cotransformed with the low copy plasmid pSEB104CD (P_{ara}::*minC minD*) or the vector pGB2 into JS964 (Δ*min*). For a control, pJB216 (P_{lac}::*minE*) was transformed together with pSEB104CD (P_{ara}::*minC minD*) into JS964. Protein expression was induced with various concentrations of IPTG (10 μM shown here) and 0.2% arabinose. Colonies of each strain grown on plates were re-suspended in 300 μl of LB and serially diluted 10-fold. 3 μl of each dilution was spotted on plates containing ampicillin, spectinomycin, arabinose and IPTG, and incubated at 37°C overnight. B) MinD^{D154A} prevents MinC/MinD copolymer formation. To assess MinC/MinD copolymerization, MinD (5 μM) and MBP-MinC^{C} (5 μM) were incubated in 50 μl reaction along with ADP or ATP (4 mM) for 10 min at 25°C. To assess inhibition by MinD^{D154A}, MinD^{D154A} (10 μM) was added to the above reactions in the presence of ADP or ATP (4 mM). The reaction mixtures were centrifuged at 175,000xg for 15 min. Supernatants and pellets were resuspended with 50 μl 2xSDS sample buffer and analyzed on 12.5% PAGE.

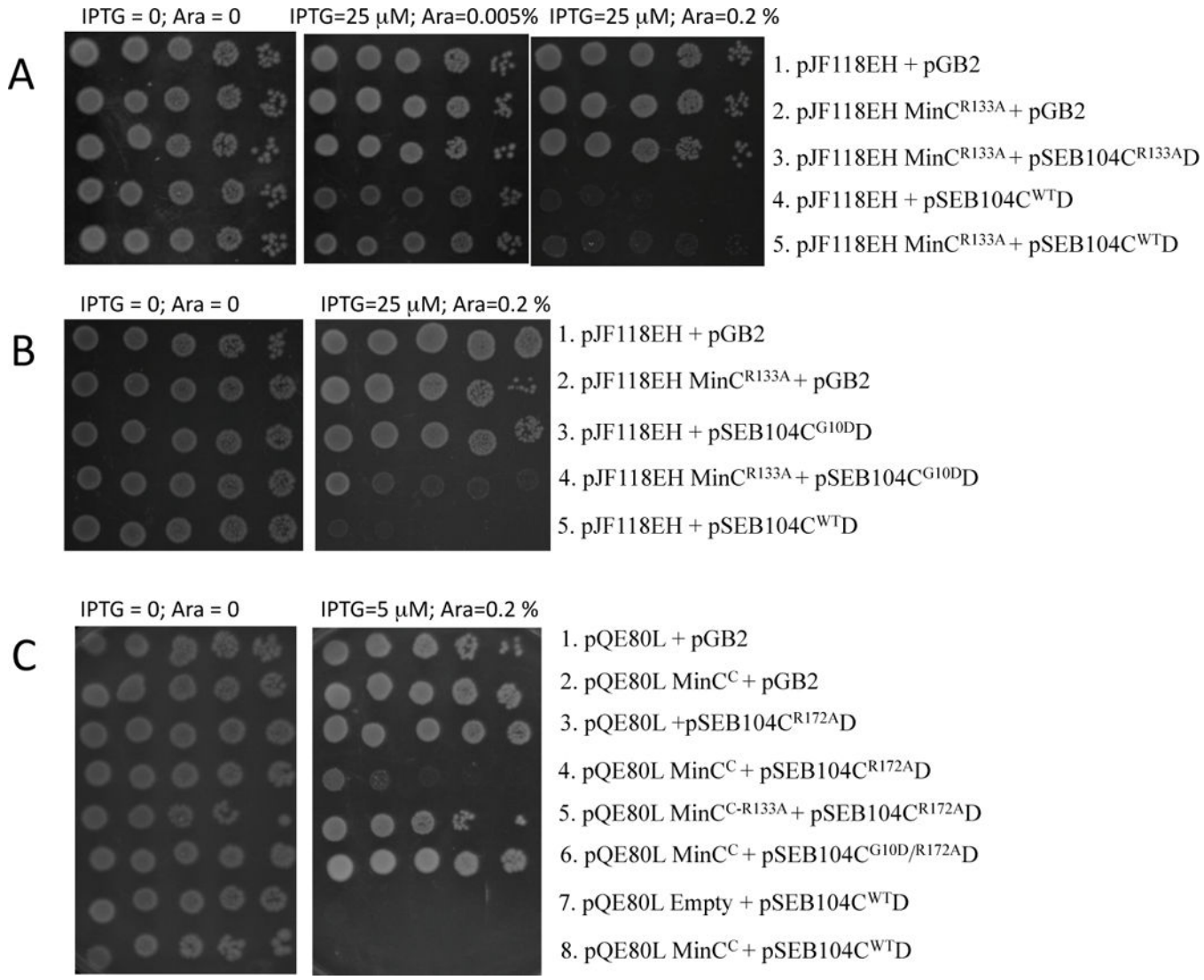

Fig. 3.

Assessing the role of MinC/MinD copolymer formation *in vivo* using MinC mutants. Spot test to assess the effect of expression of various MinC mutants unable to form copolymers on the ability of MinC to inhibit colony formation. Spot tests were performed as described in Fig. 2. Colonies were re-suspended in 300 μl of LB,serially diluted 10-fold and 3 μl of each dilution was spotted on plates containing ampicillin, spectinomycin, arabinose and IPTG, and incubated at 37°C overnight. A) Plasmid pJF118EH-MinC^{R133A} (P*tac::minC*^{R133A}) or the empty vector (pJF118EH) was cotransformed with pSEB104CD (P*ara::minC minD*), pSEB104CD (P*ara::minC*^{R133A} *minD*) or the empty vector (pGB2) into JS964 strain (Δ*min*). Expression of MinC^{R133A} and MinC/MinD or MinC^{R133A}/MinD were induced with 25 μM IPTG and 0.005 or 0.2% arabinose, respectively. Vectors were used as controls. B) Similar to A) except pJF118EHC^{R133A} (P*tac::minC*^{R133A}) was cotransformed with pSEB104C^{G10D}D (Para::*minC*^{G10D}*minD*). Induction was as in panel A. C) A plasmid containing the C-terminal domain of MinC (MinC$^{125–231}$), pQE80LC^{C} (P*T5-lac::minC*^{C}), or its derivative pQE80LC$^{C\text{-}R133A}$ (P*T5-lac::minC*$^{C\text{-}R133A}$) were cotransformed along with

pSEB104CD (Para::*minC minD*) or its derivative pSEB104C^{R172A}D (P*ara::minC*^{R172A}*minD*) into JS964 strain (Δ*min*). Protein expression was induced with 5 μM IPTG and 0.2% arabinose, respectively.

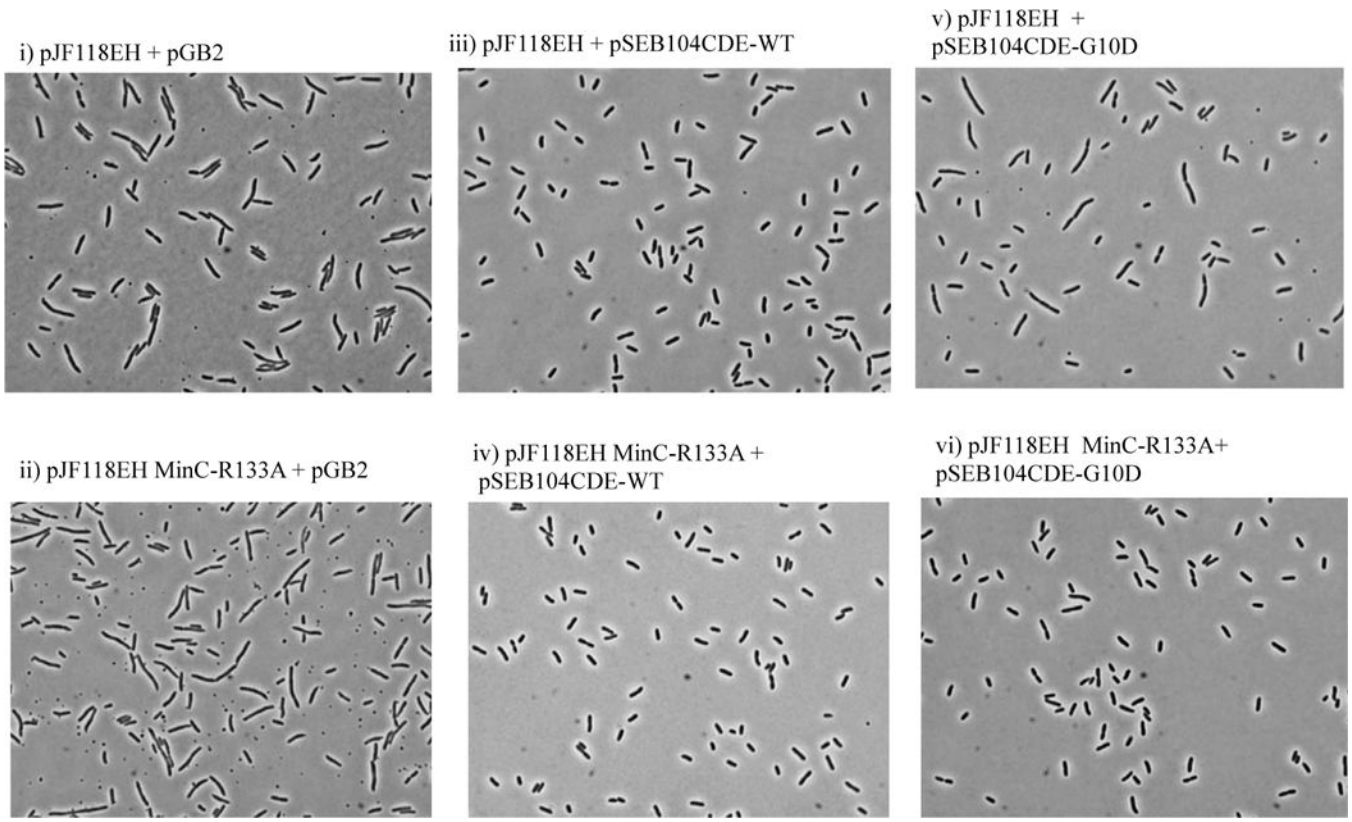

Fig. 4.

The ability of MinC mutants to form heterodimers and restore spatial regulation. A) pJF118EH (vector) or pJF118EHC^{R133A} (P_{tac}::*minC*^{R133A}) was cotransformed along with pSEB104CDE (P_{ara}::*minC minD minE*) or its derivative pSEB104C^{G10D}DE (P_{ara}::*minC*^{G10D} *minD minE*) into JS964 (Δ*min*) as described in Fig. 3. Single colonies were inoculated into LB containing ampicillin, spectinomycin, 0.2% arabinose, and 10 μM IPTG and cultured overnight at 37°C. Next day, each culture was diluted 1000-fold and grown until the mid-log phase under the same conditions. Cell morphology was examined by phase-contrast microscopy.

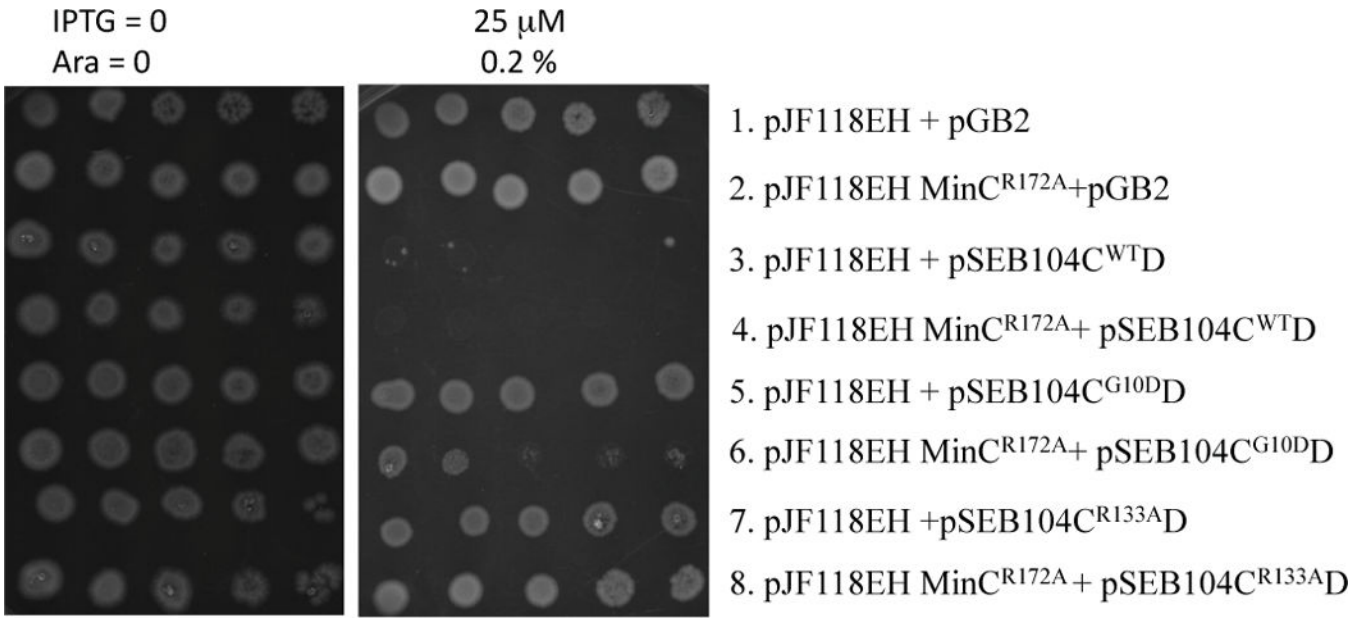

Fig. 5.

MinC interaction with the CCTP of FtsZ. A) Plasmid pJF118EHC^{R172A} (P_{tac}::*minC*^{R172A}) was cotransformed with low copy plasmid pSEB104CD (P_{ara}::*minC minD*) or its derivatives pSEB104C^{G10D}D (P_{ara}::*minC*^{G10D}*minD*) and pSEB104C^{R133A}D (P_{ara}::*minC*^{R133A}*minD*) into JS964 strain (Δ*min*). Protein induction and spot tests were carried out as described in Fig. 2A.

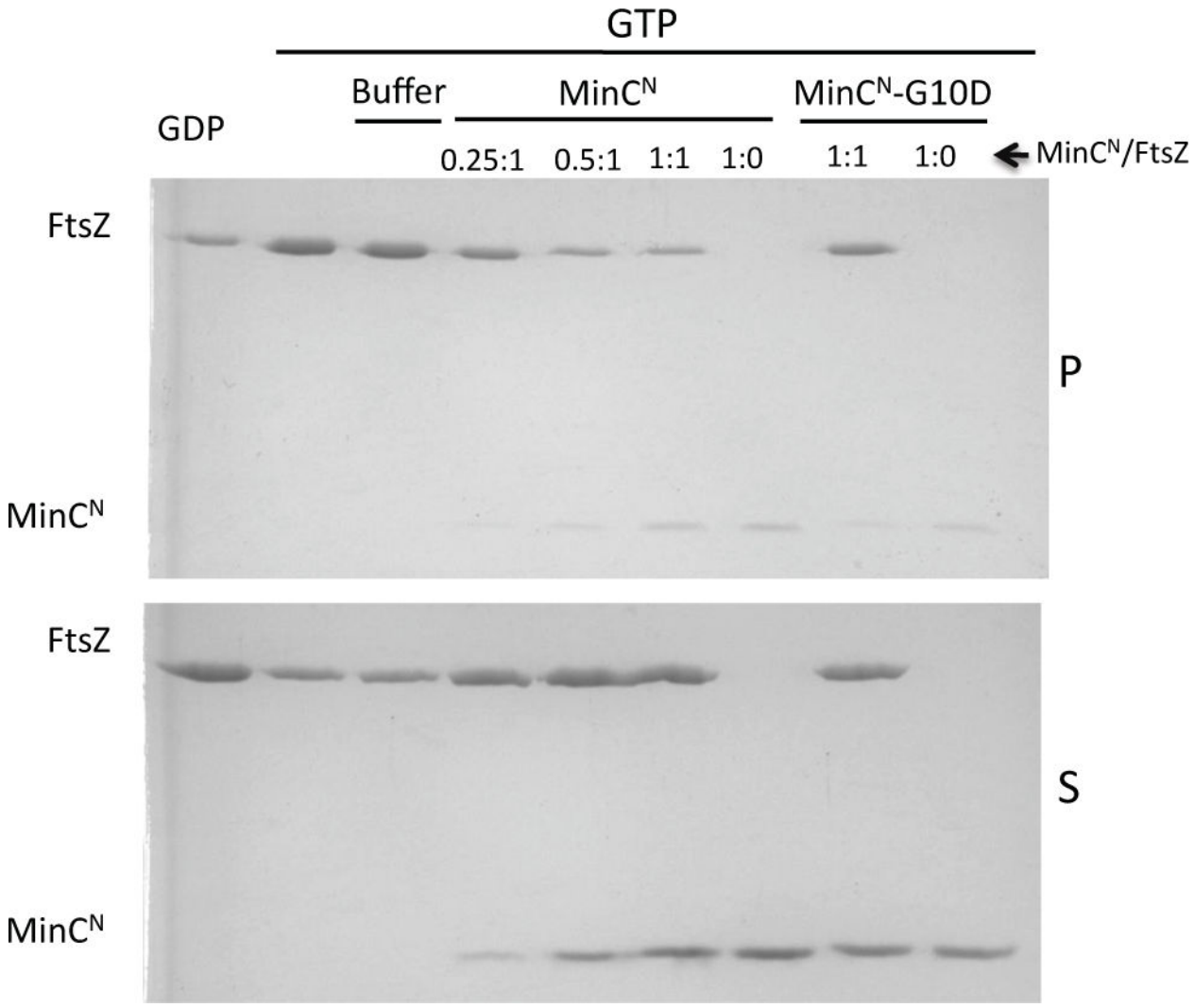

Fig. 6.

MinC^N prevents FtsZ sedimentation. A sedimentation assay was used to test the ability of MinC^N to antagonize FtsZ sedimentation. FtsZ at 5 μM was mixed with increasing concentrations of MinC^N, which has a C-terminal His tag. A control contained MinC$^{N\text{-}G10D}$ at 5 μM. The buffer contained 25 mM HEPES-NaOH [pH 6.8], 50 mM KCl, 10 mM $MgCl_2$. Reactions were initiated by the addition of 1 mM GDP or GTP and the reactions were incubated at room temperature for 5 min before centrifuging.

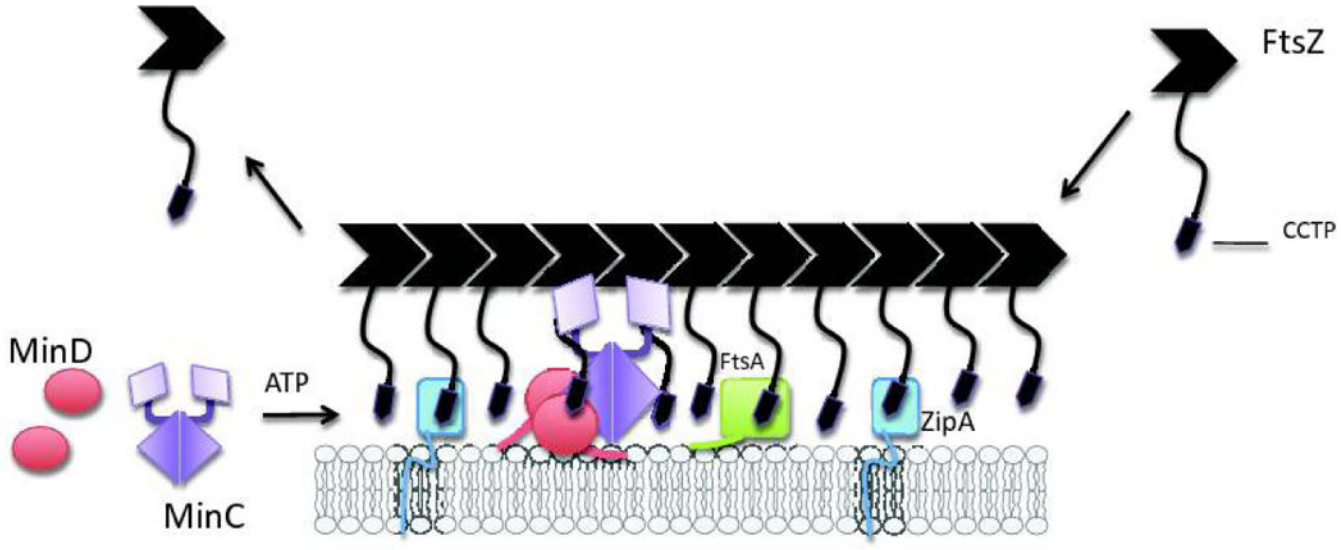

Fig. 7.

Model of MinD activation of MinC. MinD binds ATP, dimerizes and localizes to the membrane via its MTS and recruits MinC. This recruitment significantly increases the local concentration of MinC on the membrane. The MinC/MinD complex is selectively targeted to the CCTP of FtsZ filaments already tethered on the membrane by FtsA and ZipA. The $MinC^{C}$ domain bound to MinD binds the CCTP of FtsZ targeting MinC/MinD complex to the FtsZ filament. Upon $MinC^{C}$/MinD capturing the CCTP of FtsZ the $MinC^{N}$ is oriented towards the globular domains of FtsZ subunits within the filament. In this model MinC/MinD along with ZipA and FtsA prefer FtsZ filaments over monomers due to avidity. Although an individual CCTP binds the membrane localized FtsA, ZipA or MinC/MinD with low affinity an FtsZ filament binds multiple membrane partners with high affinity due to the avidity.